Proactive Dual Connectivity for Automated Guided Vehicles in Outdoor Industrial Environment

Mendoza, Jessica; Z. Kovács, István; Lechuga, Melisa Maria Lopez; Sørensen, Troels Bundgaard; Adeogun, Ramoni Ojekunle; DE-LA-BANDERA, ISABEL; Barco, Raquel

Published in:
IEEE Access

DOI (link to publication from Publisher):
10.1109/ACCESS.2022.3176730

Publication date:
2022

Document Version
Publisher's PDF, also known as Version of record

IEEE Access
Multidisciplinary ⋮ Rapid Review ⋮ Open Access Journal

Received April 27, 2022, accepted May 12, 2022, date of publication May 20, 2022, date of current version May 26, 2022.

Digital Object Identifier 10.1109/ACCESS.2022.3176730

Proactive Dual Connectivity for Automated Guided Vehicles in Outdoor Industrial Environment

JESSICA MENDOZA[1], ISTVÁN Z. KOVÁCS[2], (Member, IEEE), MELISA LÓPEZ[3], (Graduate Student Member, IEEE), TROELS B. SØRENSEN[3], (Member, IEEE), RAMONI ADEOGUN[3], (Senior Member, IEEE), ISABEL DE-LA-BANDERA[1], AND RAQUEL BARCO[1]

[1]Telecommunication Research Institute (TELMA), E.T.S. Telecommunications Engineering, University of Malaga, 29010 Malaga, Spain
[2]Nokia, 9220 Aalborg, Denmark
[3]Department of Electronic Systems, Aalborg University, 9220 Aalborg, Denmark

Corresponding author: Jessica Mendoza (jmr@ic.uma.es)

This work was supported in part by the Junta de Andalucía within project PENTA under Grant PY18-4647; and in part by the Spanish Ministry of Science, Innovation, and Universities under Grant FPU18/04786. The work of Jessica Mendoza was supported by Nokia Aalborg and Aalborg University for the research stay. The work of Ramoni Adeogun was supported by the Danish Council for Independent Research under Grant DFF 9041-00146B.

ABSTRACT 5G communication systems are one of the major enabling technologies to meet the needs of Industry 4.0. This paper focuses on the use case of automated guided vehicles (AGVs) in an outdoor industrial scenario. To meet the communication requirements in these type of use cases, dual connectivity (DC) with resource aggregation in the uplink (UL) is generally proposed. However, uncontrolled use of DC schemes may negatively affect the network causing effects such as reduced network capacity, increased signaling, and increased interference. To overcome these issues, this paper proposes and evaluates the use of a proactive DC activation algorithm based on the instantaneous quality of service (QoS) and network conditions. The proposed algorithm has two phases, a first phase in which the QoS prediction is performed, and a second phase in which the DC activation decision is made. The performance evaluation of the algorithm has been carried out in two different scenarios: a single-frequency (SF) network and a dual-frequency (DF) network; and compared to two baselines. Our results show that our predictive DC algorithm is sufficiently robust and can offer benefits in terms of reduced signaling and increased UL performance, especially in scenarios with low to medium traffic load.

INDEX TERMS Automated guided vehicles, dual connectivity, industry 4.0, proactive network management, quality of service, uplink.

I. INTRODUCTION

The industrial sector is currently facing its fourth revolution, known as Industry 4.0 [1]. This new era of industry is marked by the rise of technologies such as artificial intelligence (AI), Big Data, cyber-physical systems (CPS), and the Internet of Things (IoT). Industry 4.0 is characterized by the interconnection of machines and systems, sensorization, monitoring and control of processes, and the decentralization and automation of decision-making. The fifth generation (5G) of mobile networks is emerging as an enabling technology to meet the communication needs of new industrial applications [2]. In this context, the Third Generation Partnership Project (3GPP) has established the requirements for cyber-physical control applications for 5G communications in Industry 4.0 [3].

In industrial environments, automated guided vehicles (AGVs) are used to transport goods and materials around the manufacturing facilities. The use of AGVs improves the efficiency of logistics and material handling tasks [4]. In order to perform their functions such as collaborative tasks and human-to-machine collaboration, it is essential that the communication between these robots and their central guidance control system takes place in real time, with strict

The associate editor coordinating the review of this manuscript and approving it for publication was Olutayo O. Oyerinde.

requirements in terms of high data rates. One of the key functionalities of 5G systems for meeting these requirements is multi-connectivity (MC). In its broadest sense, MC refers to the use of multiple wireless links between the user equipment (UE) and the network. These links could be established with different base stations (BSs), with different component carriers (CCs) of the same BS, or combinations of both. The information transmitted over these links may be different, thereby increasing throughput [5], or replicas of the same data, thereby improving reliability due to the inherent diversity [6].

To meet the communication requirements of AGVs in industrial environments, we focus on the combination of two carriers in a single aggregated channel from an AGV to two different 5G nodes. This is an uplink (UL) dual connectivity (DC) scheme a.k.a. inter-site carrier aggregation (CA) or multi-flow CA [7]. The benefits provided by DC may be outweighed by its negative effects such as reduced network capacity, due to the use of resources of multiple nodes to serve the same UE, inefficient use of radio resources (transmit power and frequency resources), increased energy usage at the UE side, or increased UL interference. To mitigate these adverse effects, the use of DC should be limited to those cases in which it is absolutely necessary to meet the quality of service (QoS) requirements and the network conditions are optimal for its use (see Section I-A).

The current trend in 5G network management revolves around the use of proactive methods, capable of taking preventive actions to avoid network failures or performance degradation [8]. This is what is known as anticipatory networking. In order to anticipate the effects that different actions or events may have on the network performance, the use of predictive techniques is essential. These techniques focus on the analytics of current and past events to determine future events or behaviors [9].

In this paper, a proactive DC activation algorithm based on an industrial use case in an outdoor environment is proposed. The two-stage algorithm - QoS-prediction and DC activation - is able to proactively decide when and how to activate DC in UL.

A. RELATED WORK

MC is a key technology for improving communication aspects such as throughput, reliability and latency. In the literature, the feasibility of MC schemes in different scenarios has been proven. In [10], [11], the benefits of using inter-site CA in heterogeneous networks are investigated. A performance evaluation of UL and downlink (DL) CA in LTE-A Pro systems is presented in [12]. Authors in [5] demonstrate the advantages of combining LTE with 5G NR, and using them simultaneously to enhance the user experience through DC. In addition to the benefits of MC, the limitations and the technical challenges to be faced by using these techniques have also been presented in the literature. In [13] the challenges of using UL and DL CA in 5G are presented. The limitations of different MC schemes in industrial environments have been demonstrated in [14] by conducting measurement campaigns in factories.

Beyond these feasibility and evaluation studies, the management of MC to optimize its use while minimizing its possible adverse effects on the network has been addressed by authors in recent years. MC management has been approached from different points of view. Works such as [15]–[18] focus on secondary cell selection which is mainly based on channel quality and cell load. Different scheduling approaches to guarantee quality of service (QoS) have been proposed in [7], [19], [20]. The joint optimization of secondary cell selection with resource allocation is addressed by authors in [21], [22]. Compared to these other studies, our work focuses on deciding when and how to activate DC, i.e., deciding when it is necessary to establish a secondary link and which should be the secondary cell. Authors in [23] present an algorithm to decide when to activate UL inter-site CA based on cell load and an estimation of the potential interference to other cells. A later study [24] demonstrate that the drawbacks of DC are minimized when the reference signal received power (RSRP) from the primary and the secondary cells are similar, in this sense, users need to be within a specific DC range for DC activation. However, the solutions proposed in these works may be resource inefficient in some circumstances as DC could be activated for users who have their needs covered using single-connectivity (SC). To overcome this limitation, in [25], an heuristic method of MC activation based on the UE latency budget is presented. Here MC is activated only for those UEs that are in the DC range and present a latency budget lower than a certain threshold. While being an improvement, this mechanism does not consider the UEs' experienced QoS. Hence there could still be situations in which MC is activated for users who do not need it.

In mobile network management, predictive techniques are used to anticipate the future behavior of different network metrics, such as user location, radio link quality, traffic or QoS [26]. Depending on the prediction objective, a distinction can be made between long-term prediction [27], which aims to characterize the general trend of a signal metric, or short-term prediction [28], which focuses on predicting incremental fluctuations of the signal or metric. In this work, to anticipate when to activate DC for a given AGV, short-term QoS prediction is used. This requires a network performance sampling rate on the order of minutes, seconds, or less. The short-term prediction problem can be considered a regression problem [9]. In the field of anticipatory networking, different techniques have been proposed to address this problem. These range from simple techniques based on linear models such as auto-regressive integrated moving average (ARIMA) [29], [30], to more sophisticated ones based on the use of machine learning (ML) algorithms such as fuzzy logic [31] or artificial neural networks (ANN) [32], [33]. In the specific field of MC management in mobile networks, prediction has been used to provide seamless connectivity to users. Examples are given in [34], [35], where the position

of users is predicted to determine when a handover is needed and hence when to activate MC.

B. APPROACH AND CONTRIBUTIONS

This paper is focused on the study of a practical site-specific industrial scenario where AGVs are used for factory automation [36]. In this scenario, expanding the system bandwidth would allow increasing the number of AGVs and their moving speed. In the studied scenario, there are currently 8 AGVs moving at a speed of 1 m/s and equipped with fourth generation (4G) technology. In addition, these AGVs are moving in a limited space within the factory facility. While currently based on public radio network connectivity, we consider the case of a private industrial network configuration with optimized deployment parameters and DC option as natural upgrade, foreseeing an increased use of AGVs towards Industry 4.0. Our proposed algorithm automatically and pro-actively decides when and how to dynamically activate DC while the AGVs move along pre-determined movement paths within the industrial facility.

The key contributions of this paper can be summarized as follows.

- DC in UL for industrial AGVs: unlike most published works, this paper addresses DC management in UL, specifically the combination of two carriers in a single aggregated channel from an AGV to two network nodes; the main motivation behind this is that AGV network traffic is mostly due to UL video transmissions (see Section II-A).
- Proactive DC activation algorithm: DC activation based on QoS-prediction will limit the number of users with active DC to only those that meet certain requirements; this will avoid the excessive activation of DC seen with non-QoS-based approaches and, hence avoid the negative network-wide impact on network capacity and resource usage.
- A categorical QoS-prediction method for real network implementation: a relatively simple prediction approach based on clustering and logical regression that facilitates the integration in real network management tools is proposed.

The suitability of using predictive techniques for DC activation versus baseline mechanisms has been analyzed in different scenarios. The results show that the benefits of the proposed algorithm in terms of UL performance improvement and signaling reduction are especially relevant in scenarios with low to medium traffic load.

C. ORGANIZATION

The remainder of this paper is organized as follows. Section II presents the characteristics of the scenario and the specifications of the QoS and the DC models used. The proposed proactive DC activation algorithm is described in Section III. This algorithm consists of two stages: the categorical QoS-prediction and the DC activation. The details of the evaluation approach are presented in Section IV. It includes both the configuration of the simulations performed and the performance evaluation metrics used. The results of the performance evaluation of the proposed system are shown in Section V. Finally, the conclusions for this work are formulated in Section VI.

II. SYSTEM MODEL

A. SCENARIO

The selected network and AGV deployment scenario is depicted in Fig. 1. This corresponds to a private industrial network configuration, with optimized deployment parameters (cell locations, transmit power levels, antenna patterns, power control, etc.) where there is no impact to/from other public radio networks deployed in the same geographical area. In order to apply the DC scheme inter-site CA in our scenario, we assume that the cells depicted in Fig. 1 are implemented as remote radio heads (RRHs) and are connected to a next generation NodeB (gNB) through high bandwidth, low latency fibers. All the cells are coordinated by the same gNB.

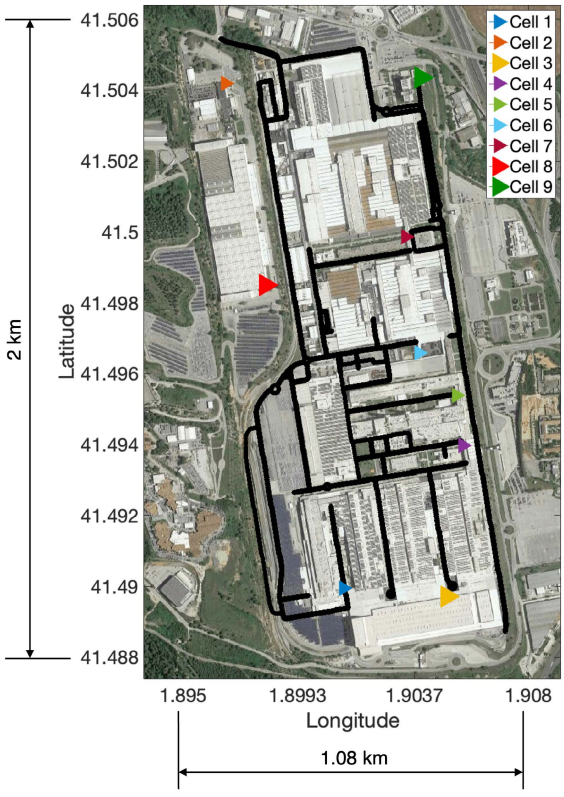

FIGURE 1. Radio cell deployment scenario. Cells 3,8,9 are either small cells or macro cells, while Cells 1,2,4,5,6,7 are small cells. AGVs movement paths are represented with black lines.

We simulated a radio network operating in the 3.5 GHz frequency band, with 100 MHz bandwidth, in time division duplex (TDD) mode, with an UL:DL split of 7:1 aligned across all cells. The large-scale radio propagation conditions are simulated with a ray-tracing tool [37] in terms of total coupling gain values along the movement paths of the AGVs

in-between the buildings. We have investigated two main network deployment scenarios:

- SF: Single-frequency network where all nine radio cells are deployed as small cells and use the full 100 MHz bandwidth. In this network deployment scenario, DC is performed following an intra-band CA scheme.
- DF: Dual-frequency network where three of the radio cells are deployed as macro cells (higher transmit power) and use 60 MHz spectrum, while the other six small cells use the remaining 40 MHz. In this network deployment scenario, DC is performed following an inter-band CA scheme.

These two cases cover the most common deployment options encountered in real-life network configurations for private, small area, mobile networks.

For their correct operation, AGVs communicate with a central guidance control system to which they send video streams in real time, and receive from it navigation control commands. Therefore, in this use case, most of the network traffic is in the UL direction. For this reason, our investigations focus on the UL traffic and service optimization when using DC. Nevertheless, for the UL connectivity to work, adequate DL connectivity has to be provided as well. Thus, the locations of the radio cells, antenna types and transmit power levels, and UL open loop power control parameters have been carefully determined, such that all AGVs experience good DL coverage with less than 1% outage (i.e., no UL/DL throughput) in the SF network and less than 2% outage in the DF network. The main radio parameters of the scenarios, as well as the main characteristics of the traffic models used in UL and DL are summarized in Table 1.

The physical movement of the AGVs is simulated with the SUMO tool [38], with a variable velocity between 0 and 8.33 m/s, and using the SUMO application jtrrouter to compute the routes based on traffic volumes and junction turning ratios. Along the movement paths, the locations of the AGVs and the corresponding coupling gain values (path loss and antenna gain), are sampled every 100 ms. The 100 ms period is also the simulation time step in our evaluations.

TABLE 1. Simulation parameters.

	Single Frequency	Dual Frequency	
Parameter	Small cells	Macro cells	Small cells
Number of cells	9	3	6
Bandwidth	100 MHz	60 MHz	40 MHz
Transmission power	23 dBm (except cell 9: 33 dBm)	46 dBm	33 dBm
Number of AGVs	30, 40, and 50	10 and 20	
Carrier frequency	3.5 GHz		
Subcarrier spacing	30 kHz		
Max. frequency allocated per AGV	30 PRBs		
BLER	10%		
Duplex mode	TDD		
AGVs max. transmission power	23 dBm (20 dBm in DC mode)		
P0-PUSCH	-95 dBm		
P0-PUSCH-Alpha	0.9		
UL AGV traffic	Video packet size: 21250 bytes Video packet periodicity: 1000/60 ms		
DL AGV traffic	Control packet size: 256 bytes Control packet periodicity: 100 ms		
DCRange	3 dB, 5 dB, and 10 dB		

B. QoS MODEL

The QoS in our studies is defined as the effective average UL transmission goodput, as estimated at medium access control (MAC) layer. The goodput metric is used instead of the throughput metric in order to account for the packet losses and re-transmissions at all lower layers, i.e. $Goodput = Throughput \cdot (1 - BLER)$, being BLER the block error rate. In our study, we use a constant BLER of 10%. The lower layer radio transmission mechanisms and signaling (link adaptation and hybrid automatic repeat request (HARQ)) are not modeled explicitly during the simulation time step. The simulated coupling gain values are used to estimate an average UL signal-to-noise-plus-interference (SINR) for each AGV in each simulation time step, which is mapped to throughput values [39]. These achieved throughput values are then converted to goodput. The UL SINR values are determined using the UE (AGV) transmit power, set based on the 3GPP specified open-loop power control formula for the physical UL shared channel (PUSCH) and the allocated UL frequency domain resources [40]. For simplicity, we use an equal UL frequency resource split between all AGVs connected to a given cell and we limit the maximum number of frequency resource blocks that can be allocated to one AGV (see Table 1).

When DC is activated, the achieved effective UL goodput is calculated as the sum of the goodput achieved on the two links, based on the corresponding UL SINR values. The UL interference due to the activation of the secondary link (wireless link between the SCell and the AGV) is explicitly considered in the calculation of the UL SINR values for all AGVs. In the case of the SF network, the interference from the secondary link affects all small cells, while in the case of the DF network, the secondary link does not impact the three macro cells.

To ensure that the video packets are delivered to the central guidance control system on time, we use a minimum latency requirement of 10 ms, leaving the 40% of the time between video packets transmissions (see Table 1) for video decoding, rendering, and refreshing [41]. The 10 ms latency requirement results in an effective goodput of 17 Mbps. This goodput value is used as the QoS requirement, and QoS outage is defined as the percentage of simulation time steps that do not meet this requirement, i.e. average goodput < 17 Mbps.

C. DUAL CONNECTIVITY MODEL

In DC, an AGV is connected simultaneously to two cells: the primary cell (PCell), and the secondary cell (SCell). As shown in Fig. 2, the serving cell or PCell receives periodic RSRP reports from the connected AGVs that are forwarded to the gNB. This information together with other performance indicators computed by the gNB such as SINR or modulation order, is used as input to the proactive DC activation algorithm. This algorithm consists of two stages. In the first stage, the QoS category prediction is performed. In the second stage, it is determined whether any action needs to be taken with respect DC (activation or deactivation). This decision is based on both the QoS category predicted in the previous stage and a given *DCRange* value. The same *DCRange* parameter value is configured for all AGVs (see Table 1). Once the DC decision is made, the PCell is in charge of forwarding the necessary signaling to the AGV to activate or deactivate DC. When DC is activated, the AGV sends video packets to the PCell and the SCell. Then, these two cells forward the packets to the gNB. The UL DC transmission can be activated at any simulation step (100 ms), for any AGV for which the UL goodput performance metrics are estimated not to meet the set QoS criteria, as long as the *DCrange* condition is met.

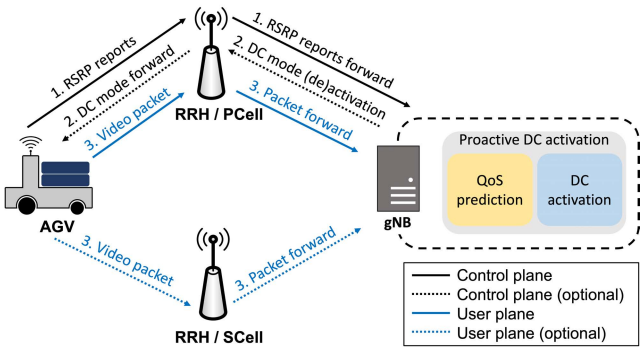

FIGURE 2. High-level diagram of the evaluated DC activation algorithm.

The AGVs can have different PCell (serving cell) and/or SCell selected in different time steps. There is no explicit mobility mechanism simulated, and in each time step, the AGVs are able to re-select the serving cell based on the strongest RSRP criteria. All AGVs are assumed to be always in radio resource control (RRC) Connected Mode. These assumptions are simple and fit the main purpose of our investigations. Considering mobility mechanisms and load balancing would improve both system and user performance, but it is not relevant for our studies as it would not impact the DC activation decisions.

III. PROACTIVE DUAL CONNECTIVITY ACTIVATION ALGORITHM

Our main target is to develop a mechanism that is able to anticipate for any AGV, in any time step t the need to activate the DC transmission in the next time step $t+1$ based on the current radio conditions and experienced QoS performance. The time horizon for our prediction can be reduced to one simulation time step (100 ms), which is long enough to assume stable average radio conditions and scheduling effects.

In our proposed proactive DC activation algorithm, called PDC, the DC activation decision is based on the estimated future fulfillment of the QoS requirement. This study proposes an algorithm for predicting whether the QoS in the next time step is above or below a set threshold value rather than attempting to predict the exact value of QoS (UL goodput value) for the next time step (100 ms). We used a categorization of the QoS based on the minimum acceptable value for the UL goodput. Thus, the QoS will have a categorical value of $y'_i = 1$ when the minimum requirement for the service is met (goodput $\geq$ 17 Mbps), and a categorical value of $y'_i = 2$ when the minimum requirement for the service is not met (goodput $<$ 17 Mbps).

In order to study the benefits of any proactive algorithm, it is important to establish and evaluate appropriate baseline mechanisms. To this end, two DC activation mechanisms have been used as baselines in this work:

- B1: Naive predictor, where the QoS performance in the current t simulation step is extrapolated and assumed to be valid for the next simulation time step, $t+1$. In this sense, the DC activation decision is based on the categorical current value (t) of the QoS, in addition to the compliance of the *DCrange*. In this case DC is activated if the categorical QoS at t is equal to 2. This is the simplest method to implement a DC activation mechanism.
- B2: 2-samples naive predictor, where the QoS performance in the previous $t-1$ and current t simulation steps are used to estimate the performance in the next simulation time step, $t+1$, resulting in a QoS categorical value of 2 when both samples ($t-1$ and t) are equal to 2. In this way, the DC activation decision is based on both the categorical current value (t) of the QoS and the value in the previous time step ($t-1$), in addition to the compliance of the *DCrange*. This method corresponds to a reactive version of the proposed method, in which a window of size 200 ms is used to check the QoS requirement.

A. PREDICTIVE QoS ALGORITHM

The QoS category prediction in our PDC algorithm, see Fig. 3, is executed in two phases: the off-line phase, in which the predictive model is trained, and the on-line phase, in which the prediction is performed using the model generated in the previous phase.

1) OFF-LINE PHASE

The off-line phase of the algorithm takes as input time series with historical data for a set of key performance indicators (KPIs), $\boldsymbol{X}$: UL SINR, UL modulation order, and number of physical resource blocks (PRBs) assigned to the AGV in UL;

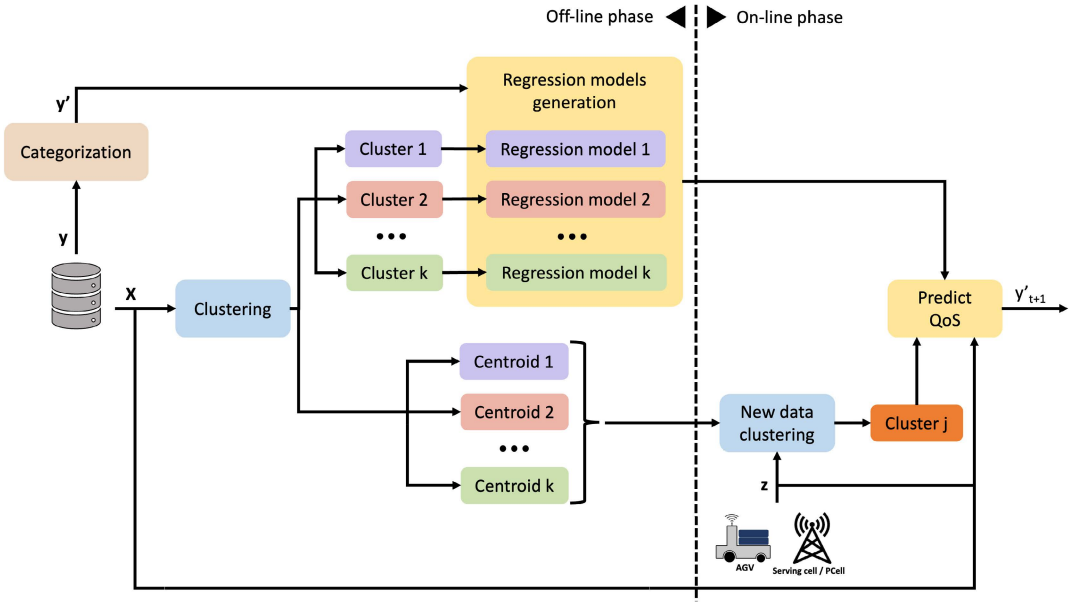

FIGURE 3. Predictive QoS algorithm diagram. $\boldsymbol{X}$ is a matrix composed of time series with historical data of the selected KPIs (UL SINR, UL modulation order, and number of PRBs assigned in UL); $\boldsymbol{y}$ is a time series with the historical values of the QoS; $\boldsymbol{y'}$ is a time series with the historical categorical values of the QoS; $\boldsymbol{z}$ is a vector with the values of the selected KPIs at the current instant (t); y'_{t+1} is the predicted categorical QoS value.

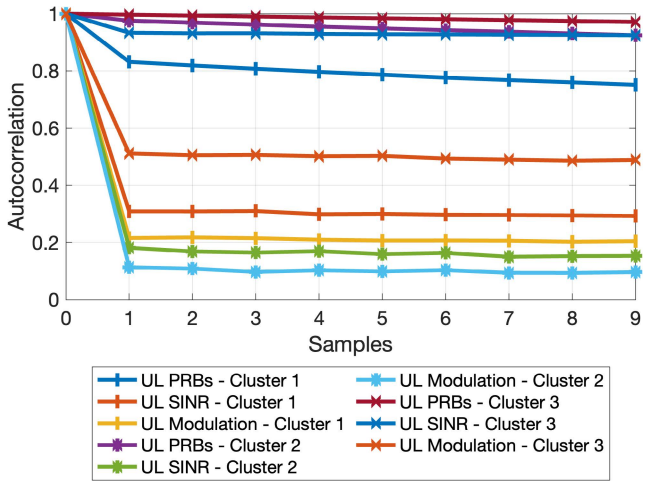

FIGURE 4. Input KPIs autocorrelation for each cluster in the SF network with 50 AGVs.

and a time series with the historical values of the QoS, i.e., UL goodput, $\boldsymbol{y}$. The selection of the KPIs used as input to the predictive model has been made based on the correlation between the different KPIs and the UL goodput. To this end, a correlation analysis has been performed for the two network deployments proposed (SF and DF) and for different number of AGVs (see Table 1). The KPIs with the highest correlation values (higher than 0.5) in the different scenarios have been selected.

As shown in Fig. 3, the first step of the predictive model is the creation of clusters, where data samples with similar values are grouped. The use of clustering as a prior step to the regression model serves to enhance the accuracy of the prediction [42]. The input data for this first step are the values of the input KPIs at each time step, $\boldsymbol{X}$. Using the k-means algorithm [43], that is one of the most widely used clustering methods, the input data is clustered. To determine the number of clusters, the silhouette value [44] is used. As an example of the different behavior of the input metrics in each cluster, Figs. 4 and 5 show the input KPIs' autocorrelation values for each cluster in the SF network with 50 AGVs and in the DF network with 20 AGVs respectively. These figures show that the behavior of the input KPIs in the different clusters are

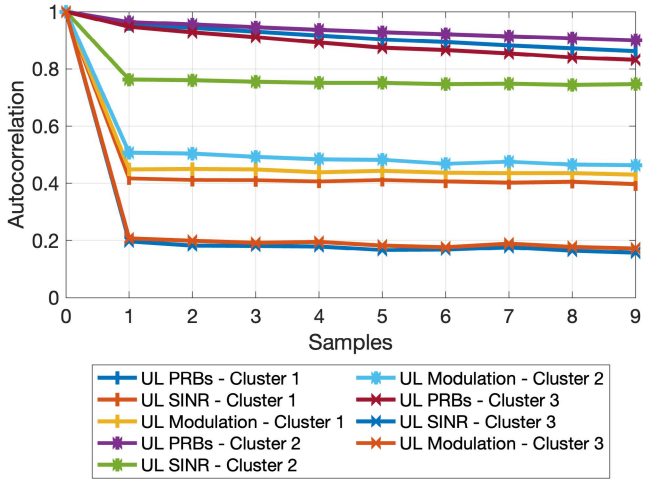

FIGURE 5. Input KPIs autocorrelation for each cluster in the DF network with 20 AGVs.

not equal. The centroids of the identified clusters are used to classify new input data in the on-line phase.

The second step of the off-line phase is the generation of regression models that estimate the category of the QoS in $t+1$. Due to the categorical characteristic of the variable to be predicted, the logistic regression technique is used [45]. The input data to this second step are the values of the KPIs in the n previous time steps to the lag to be predicted. The optimal number of past samples to use as input of the regression model in each of the different clusters has been calculated using the statistical metrics Akaike's information criteria (AIC) and bayesian information criteria (BIC). To simplify the calculation of the regression models, the same number of past samples has been used for all the regression models. In this sense, an intermediate value of the optimal number of past samples previously calculated for each cluster (5 past samples) has been used. A different logical regression model (vs. time steps) is trained for each data cluster identified in the first step.

The off-line phase of the predictive QoS algorithm, unlike the on-line phase, is executed in the original network where DC is not enabled, i.e., in an SC scenario.

2) ON-LINE PHASE

The on-line phase of the algorithm is where the real-time prediction of the categorical QoS is performed. This prediction is performed for each AGV independently. To this end, first, the AGV is assigned a cluster according to the values of the KPIs at the current instant (t), $\boldsymbol{z}$. In order to perform this cluster selection, the Euclidean distance between $\boldsymbol{z}$ and each of the clusters' centroids obtained on the off-line phase are calculated. The data belongs to the cluster that is closer (smaller Euclidean distance), represented as *Cluster j* in Fig. 3. Finally, using the regression model associated to *Cluster j*, and the current and past samples (from $t-4$ to t) of the KPIs of a given AGV, the predicted categorical QoS value, y'_{t+1}, is obtained.

B. DUAL CONNECTIVITY ACTIVATION ALGORITHM

The DC activation algorithm is in charge of making the decision about whether or not to activate DC for each AGV. This algorithm is a rule-based mechanism in which two requirements are considered. The first condition is the compliance with the configured *DCRange* parameter, i.e., that the RSRP difference between the serving cell and the strongest neighbor is less than the value set by the *DCRange* value. The second condition considered is the predicted QoS category. The QoS category check is performed using a time window that provides robustness to the algorithm, avoiding DC activation due to isolated failures or outliers. In this way, both the predicted categorical QoS value for the next time step and the current categorical QoS value are considered (i.e., window size 200 ms). DC is only activated if both samples show a degraded value (QoS category 2). Furthermore, DC activation is always performed using the strongest neighbor node, i.e., the neighbor node from which the highest RSRP is measured, as SCell. Fig. 6 shows the workflow of the algorithm.

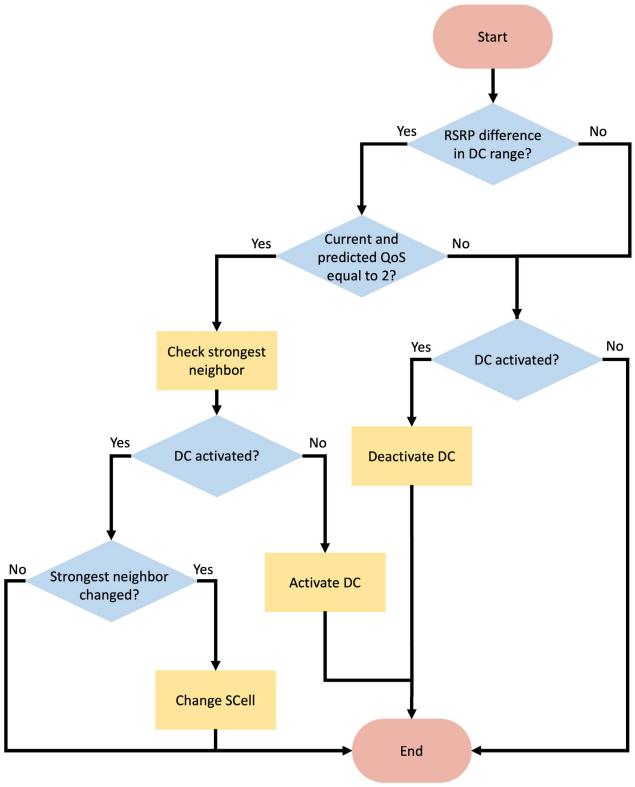

FIGURE 6. DC activation algorithm workflow.

IV. EVALUATION APPROACH

The evaluation of the proactive DC activation algorithm has been performed in the two scenarios described in Section II-A: SF and DF deployments. For this purpose, simulations of 15 minutes duration with a granularity of 100 ms have been carried out. For each of these scenarios, tests have been performed with different numbers of AGVs and using different values of the *DCrange* parameter (see Table 1). The network performance using the proposed algorithm has been compared with the network performance when using SC. To identify the optimal situations for the use of predictive techniques, the proposed predictive algorithm has been compared with the baselines (B1 and B2) presented in Subsection III-A.

A. DCrange CONFIGURATION AND TRAFFIC LOAD

The performance evaluation of the proactive DC algorithm has been carried out using different *DCrange* values: 3 dB, 5 dB, and 10 dB. The *DCrange* parameter, which indicates the maximum RSRP difference allowed to activate DC, limits the areas in which users may activate DC and, therefore, the number of AGVs with active DC at each time step. This parameter has a great impact on network performance. If the *DCrange* is set to a minimal value, the area in which DC can be activated will be reduced and very few users will be

able to benefit from this functionality. On the contrary, if the *DCrange* is set to a large value, there will be many users with DC activated at the same time, which may result in negative consequences for the network such as an increase in UL interference. In the SF network, all radio cells utilize the full available spectrum of 100 MHz, therefore the increased UL interference due to activation of DC transmissions is expected to impact the overall performance. The DF network is characterized by dividing the 100 MHz spectrum into two layers: 1) a macro cell layer composed of three macro cells using 60 MHz of the spectrum and acting as serving cells for the SC case and as PCells for the DC case; 2) a small cell layer composed of six small cells using the remaining 40 MHz and being only used as SCells for AGVs in DC. In this network, the macro cell layer will not be impacted by a large number of AGVs using DC.

Since the proposed proactive DC method relies on radio channel metrics and the derived UL goodput values, the number of AGVs is expected to impact the proactive DC algorithm performance. For a very low number of AGVs, the available radio resources are sufficient to deliver the target goodput even without using DC. Therefore, our investigations have focused on the traffic load cases with medium and high number of AGVs. In the case of SF network, evaluations have been performed in scenarios with different AGV densities: 30 AGVs, 40 AGVs, and 50 AGVs. Fig. 7 shows the UL goodput cumulative distribution function (CDF) results for these three AGV density configurations in the SF network for the SC use case. Fig. 8 shows the UL goodput CDFs in an DF network for the SC use case and with AGV densities of 10 and 20; due to the division of the spectrum in the DF network, the overall capacity is lower than in the SF network, and for this reason, the numbers of AGVs used in the DF network is lower. In a real network, a guaranteed bit rate scheduler could redistribute the excess physical resources shown in

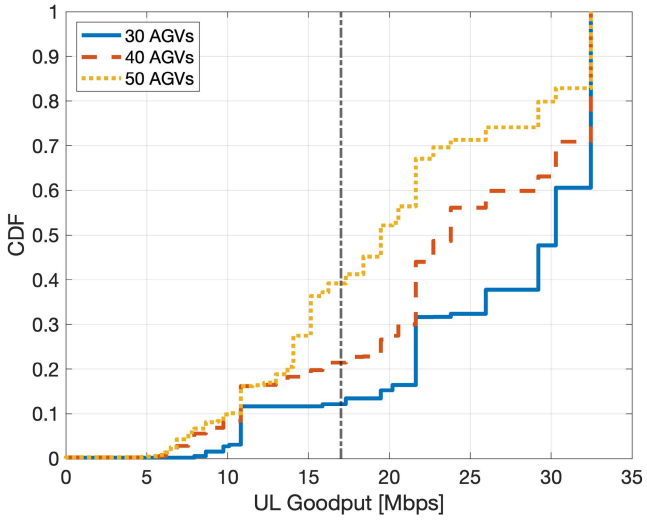

FIGURE 7. UL Goodput CDFs in the SF network for the SC use case. QoS threshold marked by vertical line at 17 Mbps.

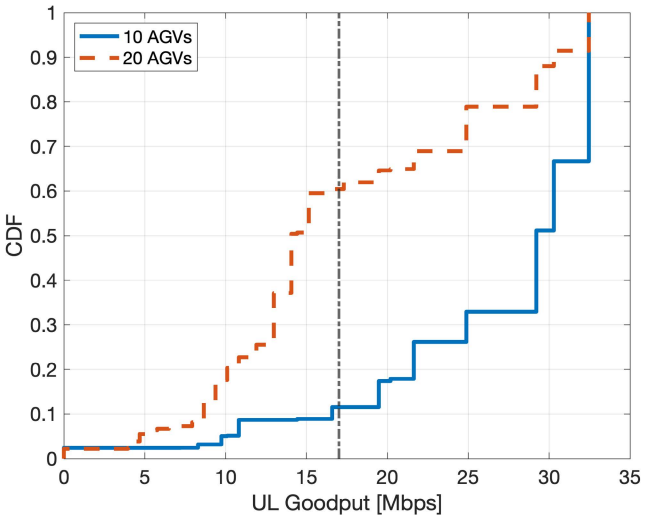

FIGURE 8. UL Goodput CDFs in the DF network for the SC use case. QoS threshold marked by vertical line at 17 Mbps.

Figs. 7 and 8 now used for UL goodput values above the QoS threshold for best-effort traffic.

To evaluate the performance of the PDC algorithm, we have performed 10 simulations for each combination of user density and *DCRange*. The original dataset is split into training (off-line phase, using 70% of the data) and evaluating (on-line phase, using 30% of the data) subsets, randomizing the sets between simulations. The DC decision algorithm is applied on the evaluation data.

B. PERFORMANCE EVALUATION METRICS

The overall performance of our proposed proactive DC activation mechanism needs to be evaluated at two levels. First, the accuracy of the QoS category predictions needs to be assessed. For this purpose, the performance of PDC is compared with the use of the baselines described in Section III, B1 and B2. The DC activation requirements considered for this evaluation are *DCrange* compliance and QoS degradation at t and $t + 1$. These different approaches are evaluated using the usual statistical metrics: false positive rate, recall, and F1 score. The impact of these metrics on the achieved radio performance is as follows:

- FPR: False positive rate, indicates the percentage of unnecessary DC activations. The radio signaling overhead due to unnecessary activation of DC is proportional to this error rate.
- Rc: Recall, indicates the proportion of times the algorithm correctly activates DC when it is needed.
- F1: F1 score, is a measure of accuracy that is calculated as the harmonic mean of precision and recall, where precision measures the proportion of times it is actually necessary to activate DC out of the total number of times DC is activated.

The second level is to evaluate the radio performance in terms of AGV (user) UL goodput gains. These results

disclose the degree of UL service improvement expected in the evaluated scenarios. In this work, the UL goodput gain is represented in terms of QoS outage, being the main objective to reduce the value of this metric for those users that under SC conditions fail to achieve the QoS requirements.

V. RESULTS AND DISCUSSION

A. SF NETWORK

1) PREDICTION ACCURACY

First, the accuracy of the QoS predictions is assessed. Table 2 shows the median values of the statistical metrics (F1, FPR, and Rc) for each of the tested scenarios. The use of the median prevents possible bias in the results due to outliers. The table shows a performance comparison between PDC and the baseline algorithms.

TABLE 2. QoS prediction assessment results in the SF network.

AGVs	*DCrange*	Algorithm	F1	FPR	Rc
30	3 dB	PDC	0.59	0.08	0.66
		B1	0.68	0.12	1
		B2	0.61	0.04	0.60
	5 dB	PDC	0.61	0.08	0.71
		B1	0.70	0.11	1
		B2	0.62	0.04	0.61
	10 dB	PDC	0.61	0.08	0.70
		B1	0.70	0.12	1
		B2	0.63	0.04	0.62
40	3 dB	PDC	0.73	0.10	0.77
		B1	0.80	0.14	1
		B2	0.77	0.05	0.76
	5 dB	PDC	0.75	0.10	0.80
		B1	0.80	0.13	1
		B2	0.77	0.06	0.76
	10 dB	PDC	0.68	0.09	0.65
		B1	0.85	0.14	1
		B2	0.82	0.05	0.82
50	3 dB	PDC	0.82	0.05	0.79
		B1	0.86	0.14	1
		B2	0.85	0.05	0.85
	5 dB	PDC	0.84	0.06	0.82
		B1	0.87	0.14	1
		B2	0.87	0.05	0.86
	10 dB	PDC	0.75	0.06	0.67
		B1	0.90	0.14	1
		B2	0.89	0.06	0.89

The first observation when analyzing F1 results is the difference in their values when comparing scenarios with different number of AGVs. It can be seen that the three methods achieve higher accuracy when the scenario is more loaded, i.e., when a higher number of AVGs is used. The higher the traffic load, the higher the autocorrelation of the QoS (UL goodput), Fig. 9, and the more predictable the QoS is, using any of the analyzed techniques.

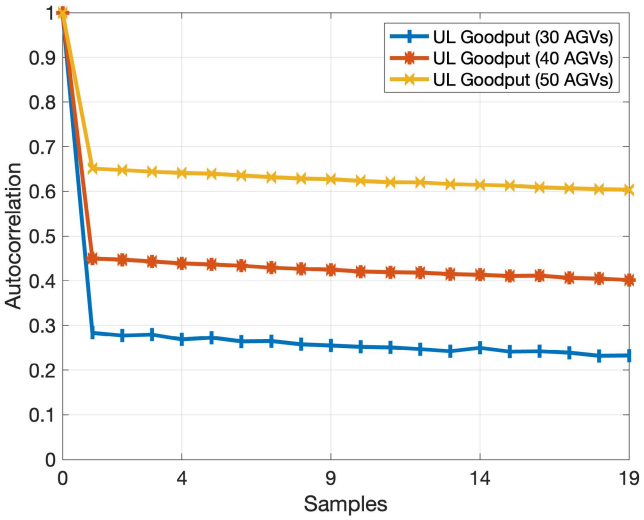

FIGURE 9. UL Goodput autocorrelation in the SF network for different number of AGVs.

The second observation is associated with the values of the *DCrange* when using the same number of AGVs in the scenario. For the results obtained using B1 and B2, there is no impact on F1 when using different *DCrange* values. However, for the case of using PDC, it can be observed that F1 drops when using a *DCrange* equal to 10 dB. As the value of the *DCrange* increases, more users can activate DC. In the SF network, this means that with DC activated, the behavior of the input KPIs (e.g., UL SINR) diverges more from their behavior in an SC scenario. Thus, PDC that is based on a predictive algorithm trained in an SC scenario, performs worse with respect to B1 and B2 when the *DCrange* is set to 10 dB. On the other hand, the fact that the overall performance of the network is negatively affected by the increase of the *DCrange* value, due to the increase of UL interference, makes the complexity of retraining the predictive model in a DC scenario undesirable.

The third observation is related to the difference in the results obtained by the three methods (PDC, B1, and B2) when using the same number of AGVs and the same *DCrange*. In this case, it can be observed that the results obtained with B1 are better than those obtained with B2 and PDC. This is due to the Rc results obtained by B1. Note that the Rc value for B1 is always 1. In B1 the QoS in the next time step $(t + 1)$ is considered to be equal to the current QoS (t) so, for the QoS in $t + 1$ to be degraded, the QoS in t must also be degraded. The QoS criterion to activate DC is that the QoS should be degraded in t and $t + 1$ (window of 200 ms). This criterion is always true when using B1, and is the reason why the false negative in B1 is always 0. F1 values of B2 and PDC are similar when the network is less loaded.

As described in Subsection IV-B, FPR indicates the percentage of unnecessary DC activations. These erroneous decisions can potentially lead to a DL signaling overload in the network, and an increase in the UL interference produced by the increase of users connected to each cell. As seen in Table 2, changes in the number of users and the value of the *DCrange* do not directly impact FPR results. However, for the different scenario configurations, method B1 presents higher FPR values, exceeding in all cases 0.1 (10%). As a consequence, this method is also the one that causes a greater signaling overhead and higher UL interference, both causing more users to be in outage due to poor radio channel quality, Fig 10. For this reason, the method B1 is discarded as a possible solution for implementing a suitable predictive DC activation method in the SF network deployment scenarios.

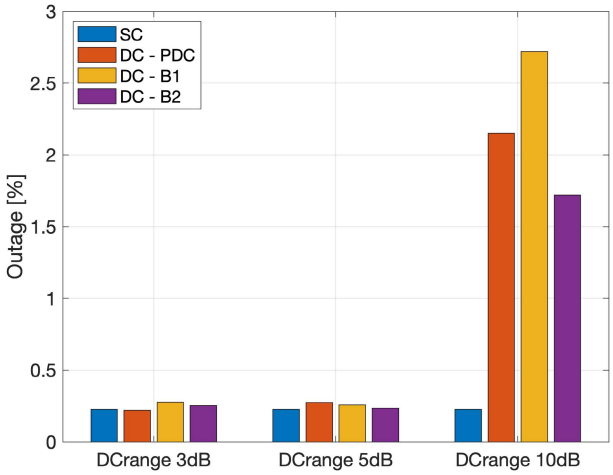

FIGURE 10. Percentage of AGVs in outage (no goodput) due to UL interference when using 40 AGVs in the SF network.

The sixth column of Table 2 shows the median of the Rc results for the tests performed. When comparing Rc results for PDC and B2 methods, it can be seen that PDC achieves better results than B2 for cases of low user density (30 AGVs). In the case of 40 AGVs the difference becomes smaller, although PDC is not the best solution in the case of using *DCrange* 10 dB. Finally, for the case of 50 AGVs, PDC fails to improve the B2 results. This is due to the high autocorrelation of the QoS in the case of using 50 AGVs (Fig. 9), which indicates that the QoS behavior is stable over time. In this context, decisions based exclusively on past samples of the QoS (B1 and B2) have a high success rate. The fact that PDC achieves better Rc results in environments with lower user density indicates that this method is more robust and does not fully rely on high spatial autocorrelation of the QoS. Finally, when comparing F1 and Rc values, there are cases where although Rc is higher for PDC than for B2, F1 is still higher for B2 than for PDC. This indicates that the precision achieved by B2 is higher than the precision obtained by PDC (as mentioned above, F1 is the harmonic mean between Rc and precision). However, to achieve better results in terms of QoS outage, it is more important to have better Rc results than precision.

2) RADIO PERFORMANCE

The performance evaluation is carried out for PDC and B2, leaving out B1 due to its high FPR. Fig. 11 shows, for each of the studied scenarios, the QoS outage achieved with PDC and B2. To calculate these outage values from the 10 simulations performed for each scenario, the samples that are susceptible to activate DC, i.e., those samples for which the *DCrange* constraint and the QoS requirements to activate DC (QoS is degraded in t and $t+1$) are met, have been used. The percentage of samples that meets these requirements in the original deployment (SC network) is shown in Table 3. As an example, Fig. 12 shows the locations where DC has been activated for an AGV during the simulations in the SF deployment with 40 AGVs and a *DCrange* value of 5 dB.

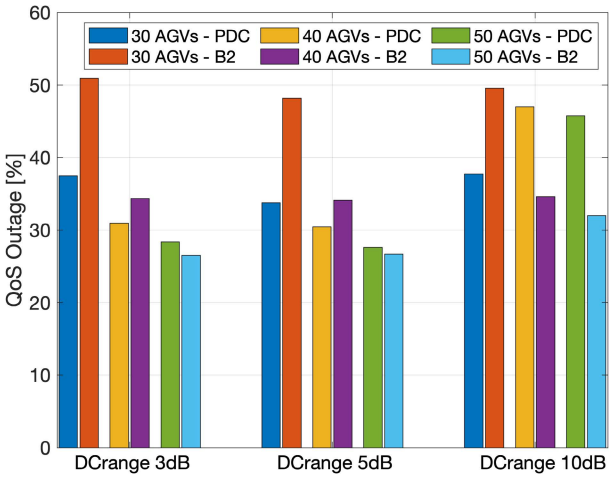

FIGURE 11. QoS outage (goodput below 17 Mbps) in the SF network.

TABLE 3. Percentage of samples susceptible to activate DC in the SF deployment.

AGVs	*DCrange*	Percentage of samples
30	3 dB	1.5%
	5 dB	2.1%
	10 dB	4.2%
40	3 dB	2.3%
	5 dB	3.3%
	10 dB	7%
50	3 dB	2.5%
	5 dB	4.3%
	10 dB	9.3%

The results in Fig. 11 support what could already be deduced from analyzing the prediction accuracy metrics. First, it can be observed that in those cases where there are 30 AGVs in the network, the PDC algorithm performs better than B2 for all three *DCrange* configuration values.

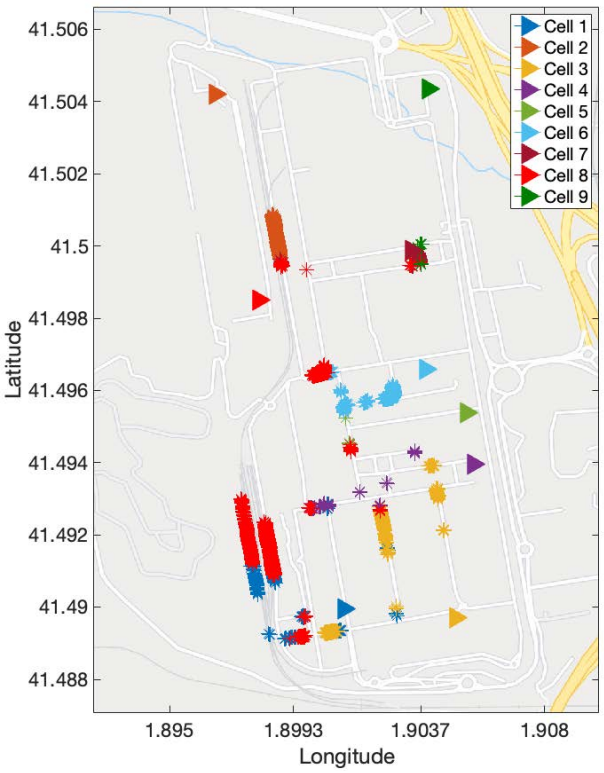

FIGURE 12. Location of the samples with DC activated during a simulation time-step in the SF network with 40 AGVs and a *DCrange* of 5 dB. The locations are represented by asterisks (*) of the same color as the cell used as PCell during the dual transmission.

In the best case (*DCrange* 5 dB), PDC leads to a 34% outage while B2 results in a 48%. When the number of AGVs in the scenario is 40, the difference in QoS outage of the two methods used becomes smaller. In the cases of *DCrange* 3 dB and 5 dB, PDC results in a 31% QoS outage while B2 leads to a 34%. In the case of *DCrange* 10 dB, the QoS outage resulting from PDC and B2 are 47% and 35% respectively. When using 50 AGVs, the PDC algorithm is not able to improve the results obtained with B2. However, the difference in QoS outage results when using *DCrange* values of 3 dB and 5 dB is small, being the 28% when using PDC and the 27% when using B2. The PDC algorithm performs better than the B2 algorithm when the QoS autocorrelation is lower. For scenarios with 40 and 50 AGVs, the PDC algorithm shows higher QoS outage when using a *DCrange* of 10 dB. This is because the number of AGVs that will potentially use DC increases in scenarios with high load and high *DCrange*, causing a worse performance of the prediction algorithm.

Based on the results shown in Fig. 10 and Fig. 11, the use *DCrange* of 10 dB is not recommended in the SF network deployment scenarios.

B. DF NETWORK

1) PREDICTION ACCURACY

Table 4 shows the medians of F1, FPR, and Rc metrics for each of the studied scenarios in the DF network. As can be seen, in general terms, the results of this table follow a similar trend to the results of Table 2. Regarding F1 (fourth column of Table 4), when comparing the results in relation to the density of AGVs, better results are achieved when the scenario is more crowded. This is due, as in the SF network case, to the higher autocorrelation of the UL goodput in this scenario, Fig. 13. In relation to the *DCrange* configurations, it can be observed that these do not directly impact the F1 results for any of the tested algorithms, including PDC. This is one of the main differences with the results obtained for the SF network. In the DF network the AGVs are initially connected to one of the three available macro cells having a single connection. When an AGV needs to activate DC at a

TABLE 4. QoS prediction assessment results in the DF network.

AGVs	*DCrange*	Algorithm	F1	FPR	Rc
10	3 dB	PDC	0.71	0.06	0.77
		B1	0.76	0.10	1
		B2	0.71	0.03	0.70
	5 dB	PDC	0.80	0.04	0.86
		B1	0.83	0.08	1
		B2	0.84	0.02	0.83
	10 dB	PDC	0.80	0.04	0.86
		B1	0.83	0.07	1
		B2	0.85	0.02	0.85
20	3 dB	PDC	0.94	0.04	0.92
		B1	0.97	0.08	1
		B2	0.97	0.03	0.97
	5 dB	PDC	0.93	0.03	0.91
		B1	0.97	0.06	1
		B2	0.98	0.02	0.98
	10 dB	PDC	0.92	0.03	0.89
		B1	0.97	0.06	1
		B2	0.98	0.02	0.98

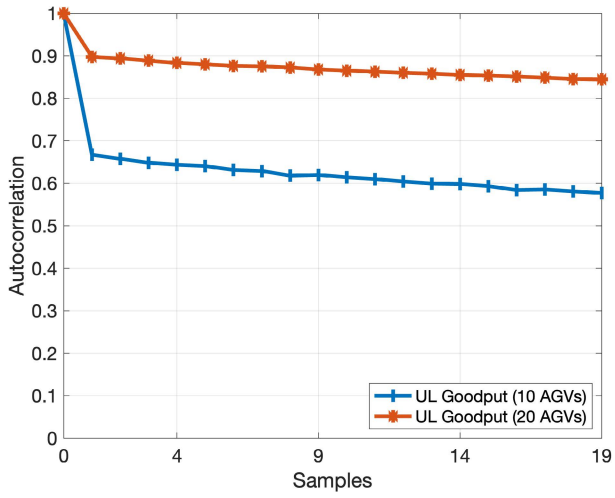

FIGURE 13. UL Goodput autocorrelation in the DF network for different number of AGVs.

given time, it will do so using one of the six available small cells deployed in the scenario. The small cells use a different part of the spectrum than the macro cells. The increase in the number of AGVs using DC simultaneously does not impact the performance of the macro cells and, therefore, neither the performance of PDC based on a predictive algorithm trained in an SC scenario.

The fifth column of Table 4 shows the FPR results obtained for the different setups in the DF network. For the three methods (PDC, B1, and B2), the FPR results are reduced with respect to those obtained in the SF network. Although in this case the results of FPR obtained with B1 do not exceed 0.1 for all scenarios, they are almost three times those obtained by B2 and double in most cases the results obtained with PDC. Having a higher FPR leads to a higher signaling overhead in the network, due to the signaling produced by activating/deactivating DC when it is not necessary. However, in the DF network the increase in UL interference only occurs in the small cell layer. No degradation of network performance is observed, since the small cells are not heavily loaded. Fig. 14 shows the percentage of AGVs in outage due to poor UL radio channel conditions. The use of DC allows reducing the number of AGVs that cannot transmit in the SC network.

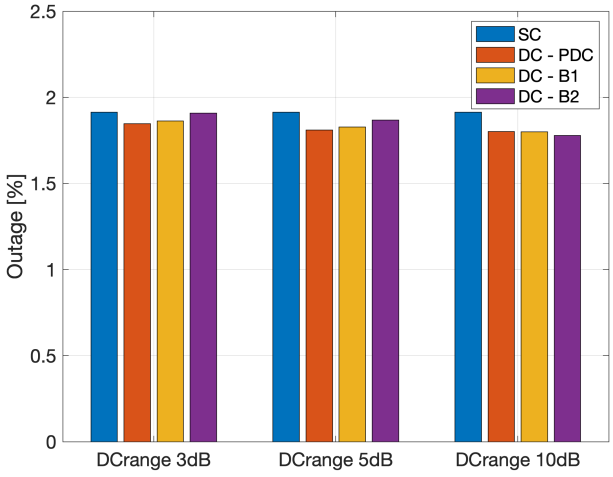

FIGURE 14. Percentage of AGVs in outage (no goodput) due to UL interference when using a 10 AGVs in the DF network.

To conclude with the assessment of the QoS prediction in the DF network, the Rc metric is analyzed (sixth column of Table 4). These results follow the same trend as those obtained for the SF network. It can be observed that, due to the behavior of the B1 method and the QoS criteria defined for DC activation in the proposed algorithm, the Rc for B1 is always equal to 1. When comparing the results of the PDC and B2 methods, it can be observed that PDC obtains better results for scenarios with less user load, indicating that this method is more robust than B2 in situations where the QoS autocorrelation is low.

2) RADIO PERFORMANCE

Fig. 15 shows the QoS outage results for the PDC and B2 methods. As in the SF network, to calculate these values, only the samples that are susceptible to activate DC, i.e., those samples for which the *DCrange* constraint and the QoS requirements to activate DC (QoS is degraded in t and $t + 1$) are met, have been used. The percentage of samples that meets these requirements in the original deployment (SC network) is shown in Table 5. As an example, Fig. 16 shows the locations where DC has been activated for an AGV during the simulations in the DF deployment with 10 AGVs and a *DCrange* value of 5 dB.

Fig. 15 shows that, for the scenarios with lower user density (10 AGVs), the QoS outage resulting from the PDC algorithm is between 18% (for *DCrange* of 3 dB) and 11% (for *DCrange* of 5 dB and 10 dB) while the QoS outage araising from B2 is between 31% (for *DCrange* of 3 dB) and 16% (for *DCrange* of 5 dB and 10 dB). In the network with 20 AGVs, where the QoS is more autocorrelated, the QoS outage resulting from PDC, although presenting very low values being less than 10% for the three *DCrange* values tested and leads to a 7% in the case of use a *DCrange* of 3 dB, does not improve the results of B2.

A key difference compared to the results obtained for SF networks, based on the results shown in Fig. 14 and Fig. 15, the use *DCrange* of 10 dB is suitable for DF network deployment scenarios. In addition, due to the lower UL interference produced in this scenario when using DC, the UL goodput gain in it is higher (lower QoS outage) than in the SF deployment.

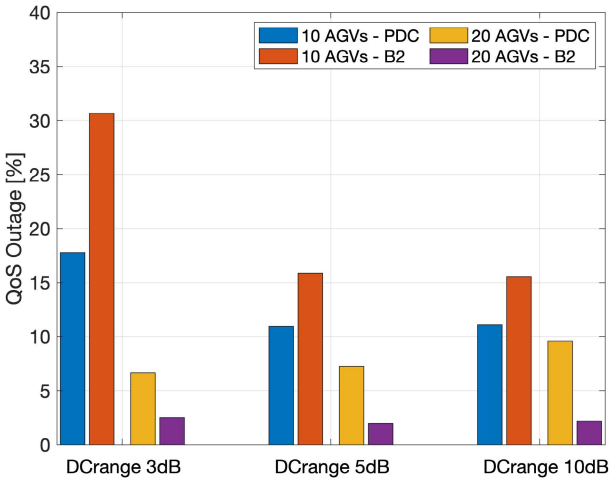

FIGURE 15. QoS outage (goodput below 17 Mbps) in the DF network.

TABLE 5. Percentage of samples susceptible to activate DC in the DF deployment.

AGVs	*DCrange*	Percentage of samples
10	3 dB	9.6%
	5 dB	10.4%
	10 dB	12.3%
20	3 dB	23.2%
	5 dB	25.6%
	10 dB	31.4%

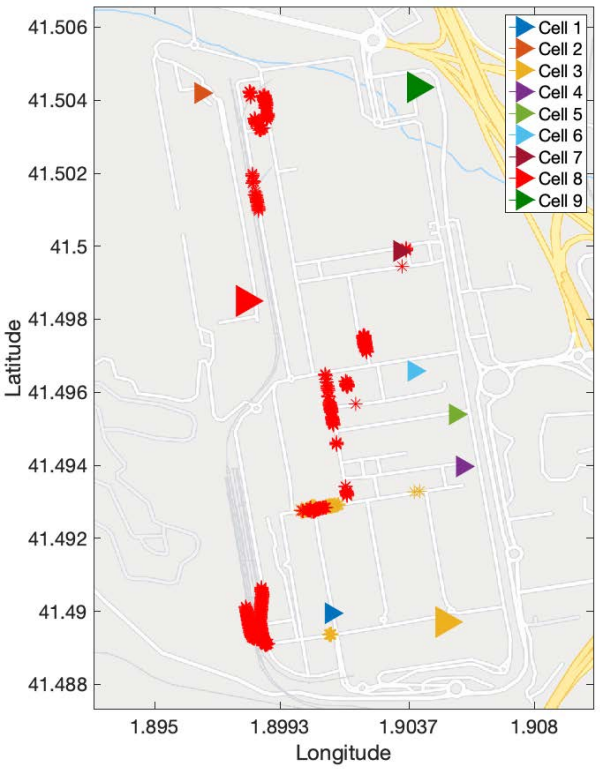

FIGURE 16. Location of the samples with DC activated during a simulation time-step in the DF network with 10 AGVs and a *DCrange* of 5 dB. The locations are represented by asterisks (*) of the same color as the cell used as PCell during the dual transmission.

VI. CONCLUSION

This paper presents a proactive uplink dual-connectivity (PDC) activation management algorithm for the use case of AGVs in an outdoor industrial scenario. The proposed algorithm can automatically make decisions about DC activation/deactivation based on the predicted QoS and the RSRP difference between the PCell and the SCell (*DCrange* value). For this purpose, the algorithm is composed of two stages: in the first step, a prediction of the QoS category is performed, with respect to a set threshold level; in the second step, the DC activation decision is made by using a rule-based mechanism. The performance evaluation of the proposed solution has been carried out in a simulated realistic outdoor industrial environment using two different network deployments: single-frequency (SF) network and dual-frequency (DF) network, as well as different configurations in terms of the number of AGVs in the network (load) and of the *DCrange* values. The performance of the proposed algorithm has been compared with the performance of two baseline reactive algorithms: 1-step naive predictor (B1) and 2-samples naive predictor (B2). B1 corresponds to simple method reactive DC activation mechanism and is used in most of the DC studies found in the literature; while B2 corresponds to a reactive version of our proposed method. The results in low-medium load conditions show that, when the *DCrange* constraint and the QoS requirements to activate DC are met, the proposed PDC algorithm reduces the QoS outage (UL throughput below target) compared to B1 and B2 to 31% in the SF deployment and to 11% in the DF deployment. In high load conditions, the performance of the PDC algorithm is generally on pair with the B2 performance, with slight dependency on the *DCrange* value. In addition, the proposed PDC algorithm shows a lower false positive rate in DC activation compared to B1 and slightly higher rates compared to B2, depending on the load. Therefore, the PDC algorithm reduces unnecessary DL signaling associated with DC activation/deactivation and lowers the number of failed transmissions due to poor UL radio channel conditions. Finally, the proposed PDC algorithm was shown to have good performance in scenarios with low QoS autocorrelation (time domain), thus being more robust to changing radio environment and interference conditions compared to the baseline algorithms. Our setup and evaluations presented in this paper addressed DC in the context of transmission with carrier aggregation for the purpose of improving the uplink throughput. Nevertheless, we consider that a similar predictive algorithm can be beneficially applied also for packet duplication transmission schemes, and in this case the QoS metric improved is the reliability of the uplink transmissions.

ABBREVIATIONS

The following abbreviations are used in this manuscript:

3GPP	Third Generation Partnership Project
4G	Fourth generation
5G	Fifth generation
AGV	Automated guided vehicle
AI	Artificial intelligence
ANN	Artificial neural network
ARIMA	Autoregressive integrated moving average
B1	Baseline Naive predictor
B2	Baseline 2-samples naive predictor
BLER	Block error rate
BS	Base station
CA	Carrier aggregation
CC	Component carrier
CPS	Cyber-physical systems
DC	Dual connectivity
DF	Dual-frequency
DL	Downlink
F1	F1 score
FPR	False positive rate
gNB	Next generation NodeB
HARQ	Hybrid automatic repeat request
IoT	Internet of things
KPI	Key performance indicator
MAC	Medium access control
MC	Multi-connectivity
ML	Machine learning
PCell	Primary cell
PDC	Proactive dual-connectivity
PRB	Physical resource block
PUSCH	Physical uplink shared channel

QoS	Quality of service
Rc	Recall
RRC	Radio resource control
RRH	Remote radio head
RSRP	Reference signal received power
SC	Single connectivity
SCell	Secondary cell
SF	Single-frequency
SINR	Signal-to-noise-plus-interference
TDD	Time division duplex
UE	User equipment
UL	Uplink

REFERENCES

[1] M. Wollschlaeger, T. Sauter, and J. Jasperneite, "The future of industrial communication: Automation networks in the era of the Internet of Things and Industry 4.0," *IEEE Ind. Electron. Mag.*, vol. 11, no. 1, pp. 17–27, Mar. 2017.

[2] J. Bedo, E. Strinati, S. Castellvi, T. Cherif, M. Frascolla, W. Haerick, I. Korthals, O. Lazaro, E. Sutedjo, and L. Usatorre, "5G and the factories of the future," Haerick, Wouter ve Gupta, Milon, Editörler, White Paper, 2015. Accessed: May 20, 2022. [Online]. Available: https://5g-ppp.eu/wp-content/uploads/2014/02/5G-PPP-White-Paper-on-Factories-of-the-Future-Vertical-Sector.pdf and https://5g-ppp.eu/white-papers/

[3] *Service Requirements for Cyber-Physical Control Applications in Vertical Domains (Release 17)*, document 3GPP TS 22.104, TR V17.4.0, Sep. 2020.

[4] E. A. Oyekanlu, A. C. Smith, W. P. Thomas, G. Mulroy, D. Hitesh, M. Ramsey, D. J. Kuhn, J. D. Mcghinnis, S. C. Buonavita, N. A. Looper, M. Ng, A. Ng'oma, W. Liu, P. G. Mcbride, M. G. Shultz, C. Cerasi, and D. Sun, "A review of recent advances in automated guided vehicle technologies: Integration challenges and research areas for 5G-based smart manufacturing applications," *IEEE Access*, vol. 8, pp. 202312–202353, 2020.

[5] M. U. Sheikh, M. Z. Asghar, and R. Jäntti, "Dual connectivity in non-stand alone deployment mode of 5G in Manhattan environment," in *Proc. Int. Conf. Electron., Inf., Commun. (ICEIC)*, Jan. 2020, pp. 1–4.

[6] J. Rao and S. Vrzic, "Packet duplication for URLLC in 5G dual connectivity architecture," in *Proc. IEEE Wireless Commun. Netw. Conf. (WCNC)*, Apr. 2018, pp. 1–6.

[7] A. Alorainy, "Buffer-aware packet scheduling in multi-flow carrier aggregation," in *Proc. IEEE Int. Conf. Commun. (ICC)*, Jun. 2020, pp. 1–7.

[8] E. Bastug, M. Bennis, and M. Debbah, "Living on the edge: The role of proactive caching in 5G wireless networks," *IEEE Commun. Mag.*, vol. 52, no. 8, pp. 82–89, Aug. 2014.

[9] P. Chakraborty, M. Corici, and T. Magedanz, "A comparative study for time series forecasting within software 5G networks," in *Proc. 14th Int. Conf. Signal Process. Commun. Syst. (ICSPCS)*, Dec. 2020, pp. 1–7.

[10] H. Wang, C. Rosa, and K. I. Pedersen, "Dedicated carrier deployment in heterogeneous networks with inter-site carrier aggregation," in *Proc. IEEE Wireless Commun. Netw. Conf. (WCNC)*, Apr. 2013, pp. 756–760.

[11] A. Alorainy and M. J. Hossain, "Cross-layer performance analysis of downlink multi-flow carrier aggregation in heterogeneous networks," *IEEE Access*, vol. 7, pp. 23303–23318, 2019.

[12] A. Kolackova, S. Saafi, P. Masek, J. Hosek, and J. Jerabek, "Performance evaluation of carrier aggregation in LTE—A pro mobile systems," in *Proc. 43rd Int. Conf. Telecommun. Signal Process. (TSP)*, Jul. 2020, pp. 627–632.

[13] Nidhi, A. Mihovska, and R. Prasad, "Overview of 5G new radio and carrier aggregation: 5G and beyond networks," in *Proc. 23rd Int. Symp. Wireless Pers. Multimedia Commun. (WPMC)*, Oct. 2020, pp. 1–6.

[14] E. J. Khatib, D. A. Wassie, G. Berardinelli, I. Rodriguez, and P. Mogensen, "Multi-connectivity for ultra-reliable communication in industrial scenarios," in *Proc. IEEE 89th Veh. Technol. Conf. (VTC-Spring)*, Apr. 2019, pp. 1–6.

[15] M. Giordani, M. Mezzavilla, S. Rangan, and M. Zorzi, "An efficient uplink multi-connectivity scheme for 5G millimeter-wave control plane applications," *IEEE Trans. Wireless Commun.*, vol. 17, no. 10, pp. 6806–6821, Oct. 2018.

[16] D. Guzman, R. Schoeffauer, and G. Wunder, "Predictive network control in multi-connectivity mobility for URLLC services," in *Proc. IEEE 24th Int. Workshop Comput. Aided Model. Design Commun. Links Netw. (CAMAD)*, Sep. 2019, pp. 1–7.

[17] V. Poirot, M. Ericson, M. Nordberg, and K. Andersson, "Energy efficient multi-connectivity algorithms for ultra-dense 5G networks," *Wireless Netw.*, vol. 26, no. 3, pp. 2207–2222, Apr. 2020.

[18] I. de la Bandera, D. Palacios, and R. Barco, "Multinode component carrier management: Multiconnectivity in 5G," *IEEE Veh. Technol. Mag.*, vol. 16, no. 2, pp. 40–47, Jun. 2021.

[19] B.-J. Chang and W.-T. Chang, "Cost-Reward-based carrier aggregation with differentiating network slicing for optimizing radio RB allocation in 5G new radio network," in *Proc. IEEE 10th Annu. Inf. Technol., Electron. Mobile Commun. Conf. (IEMCON)*, Oct. 2019, pp. 0813–0819.

[20] H. M. Zegallai and S. A. Awad, "Packet scheduling with carrier aggregation for balancing QoS in LTE advanced networks," in *Proc. IEEE 1st Int. Maghreb Meeting Conf. Sci. Techn. Autom. Control Comput. Eng. (MI-STA)*, May 2021, pp. 882–886.

[21] R. Joda, M. Elsayed, H. Abou-Zeid, R. Atawia, A. B. Sediq, G. Boudreau, and M. Erol-Kantarci, "QoS-aware joint component carrier selection and resource allocation for carrier aggregation in 5G," in *Proc. IEEE Int. Conf. Commun.*, Jun. 2021, pp. 1–6.

[22] W. Gao, L. Ma, and G. Chuai, "Joint optimization of component carrier selection and resource allocation in 5G carrier aggregation system," *Phys. Commun.*, vol. 25, pp. 293–297, Dec. 2017. [Online]. Available: https://www.sciencedirect.com/science/article/pii/S1874490716301884

[23] H. Wang, C. Rosa, and K. I. Pedersen, "Uplink inter-site carrier aggregation between macro and small cells in heterogeneous networks," in *Proc. IEEE 80th Veh. Technol. Conf. (VTC-Fall)*, Sep. 2014, pp. 1–5.

[24] N. H. Mahmood, M. Lopez, D. Laselva, K. Pedersen, and G. Berardinelli, "Reliability oriented dual connectivity for URLLC services in 5G new radio," in *Proc. 15th Int. Symp. Wireless Commun. Syst. (ISWCS)*, Aug. 2018, pp. 1–6.

[25] N. H. Mahmood and H. Alves, "Dynamic multi-connectivity activation for ultra-reliable and low-latency communication," in *Proc. 16th Int. Symp. Wireless Commun. Syst. (ISWCS)*, Aug. 2019, pp. 112–116.

[26] N. Bui, M. Cesana, S. A. Hosseini, Q. Liao, I. Malanchini, and J. Widmer, "A survey of anticipatory mobile networking: Context-based classification, prediction methodologies, and optimization techniques," *IEEE Commun. Surveys Tuts.*, vol. 19, no. 3, pp. 1790–1821, Apr. 2017.

[27] Y. Yu, J. Wang, M. Song, and J. Song, "Network traffic prediction and result analysis based on seasonal ARIMA and correlation coefficient," in *Proc. Int. Conf. Intell. Syst. Design Eng. Appl.*, vol. 1, Oct. 2010, pp. 980–983.

[28] L. Fang, X. Cheng, H. Wang, and L. Yang, "Mobile demand forecasting via deep graph-sequence spatiotemporal modeling in cellular networks," *IEEE Internet Things J.*, vol. 5, no. 4, pp. 3091–3101, Aug. 2018.

[29] Y. Shu, "Wireless traffic modeling and prediction using seasonal ARIMA models," *IEICE Trans. Commun.*, vol. 88, no. 10, pp. 3992–3999, Oct. 2005.

[30] B. Zhou, D. He, and Z. Sun, "Traffic modeling and prediction using ARIMA/GARCH model," in *Modeling and Simulation Tools for Emerging Telecommunication Networks*. Cham, Switzerland: Springer, 2006, pp. 101–121.

[31] H. Qu, Y. Zhang, J. Zhao, G. Ren, and W. Wang, "A hybrid handover forecasting mechanism based on fuzzy forecasting model in cellular networks," *China Commun.*, vol. 15, no. 6, pp. 84–97, Jun. 2018.

[32] D. Ferreira, A. B. Reis, C. Senna, and S. Sargento, "A forecasting approach to improve control and management for 5G networks," *IEEE Trans. Netw. Service Manage.*, vol. 18, no. 2, pp. 1817–1831, Jun. 2021.

[33] C. Zhang, P. Patras, and H. Haddadi, "Deep learning in mobile and wireless networking: A survey," *IEEE Commun. Surveys Tuts.*, vol. 21, no. 3, pp. 2224–2287, 3rd Quart., 2019.

[34] K. Qi, T. Liu, C. Yang, S. Suo, and Y. Huang, "Dual connectivity-aided proactive handover and resource reservation for mobile users," *IEEE Access*, vol. 9, pp. 36100–36113, 2021.

[35] C. Wang, Z. Zhao, Q. Sun, and H. Zhang, "Deep learning-based intelligent dual connectivity for mobility management in dense network," in *Proc. IEEE 88th Veh. Technol. Conf. (VTC-Fall)*, Aug. 2018, pp. 1–5.

[36] *Robots Take to the Streets*. Accessed: May 20, 2022. [Online]. Available: https://www.seat.com/company/news/cars/robots-take-to-the-streets.html

[37] *WinProp Manual for Version 2018.1.2 Release*. Accessed: May 20, 2022. [Online]. Available: https://altairhyperworks.com/product/FEKO/WinProp-Propagation-Modeling

[38] *SUMO User Documentation*. Accessed: May 20, 2022. [Online]. Available: https://www.eclipse.org/sumo
[39] *User Equipment (UE) Radio Access Capabilities (Release 16)*, document 3GPP TS 38.306, TR V 16.3.0, Jan. 2021.
[40] *Physical Layer Procedures for Control (Release 16)*, document 3GPP TS 38.213, TR V16.3.0, Oct. 2020.
[41] H. Wang, X. Zhang, H. Chen, Y. Xu, and Z. Ma, "Inferring end-to-end latency in live videos," *IEEE Trans. Broadcast.*, early access, Apr. 12, 2021, doi: 10.1109/TBC.2021.3071060.
[42] S. Trivedi, Z. A. Pardos, and N. T. Heffernan, "The utility of clustering in prediction tasks," 2015, *arXiv:1509.06163*.
[43] D. Arthur and S. Vassilvitskii, "k-means++: The advantages of careful seeding," Stanford Univ., Stanford, CA, USA, Tech. Rep. 778, Jun. 2006. Accessed: May 20, 2022. [Online]. Available: http://ilpubs.stanford.edu:8090/778/
[44] P. J. Rousseeuw, "Silhouettes: A graphical aid to the interpretation and validation of cluster analysis," *J. Comput. Appl. Math.*, vol. 20, no. 1, pp. 53–65, Jan. 1987.
[45] A. J. Dobson and A. G. Barnett, *An Introduction to Generalized Linear Models*. Boca Raton, FL, USA: CRC Press, 2018.

JESSICA MENDOZA received the B.S. degree in telematics engineering and the M.S. degree in telematics and telecommunication networks from the University of Malaga, in 2017 and 2018, respectively, where she is currently pursuing the Ph.D. degree. In 2017, she joined the Department of Communications Engineering, University of Malaga, through an investigation internship where she continues working as a Research Assistant. Her research interests include automation of mobile networks management tasks, specifically in network self-optimization and self-healing areas.

ISTVÁN Z. KOVÁCS (Member, IEEE) received the B.Sc. degree from the Politehnica University of Timişoara, Romania, in 1989, the M.Sc. degree in electrical engineering from the École Nationale Supérieure des Télécommunications de Bretagne, France, in 1996, and the Ph.D. degree in electrical engineering (wireless communications) from Aalborg University, Aalborg, Denmark, in 2002. He is currently working as a Senior Research Engineer at Nokia, Aalborg, where he conducts standardization research on machine learning-driven radio resource management and on radio connectivity enhancements for non-terrestrial and aerial vehicle communications, in LTE and 5G networks.

MELISA LÓPEZ (Graduate Student Member, IEEE) received the B.Sc. and M.Sc. degrees in telecommunications engineering from the Universitat Politécnica de Catalunya, Spain, in 2016 and 2018, respectively. She is currently pursuing the Ph.D. degree in wireless communications with Aalborg University, Denmark. Her research interests include radio propagation, field measurements, and multi-connectivity.

TROELS B. SØRENSEN (Member, IEEE) received the M.Sc. degree in electrical engineering, in 1990, and the Ph.D. degree in wireless communications from Aalborg University, in 2002. He worked with type approval test methods as part of ETSI standardization activities. Since 1997, he has been with Aalborg University, where he is currently an Associate Professor with the Wireless Communication Networks Section. He has successfully supervised more than 15 Ph.D. students and published more than 120 journals and conference papers. He has participated to several European projects, latest acting as the coordinator of the SESAR JU research project Drone Critical Communications (DroC2om). His teaching and research interests include cellular network performance and evolution, radio resource management, propagation characterization, and related experimental activities.

RAMONI ADEOGUN (Senior Member, IEEE) received the B.Eng. degree in electrical and computer engineering from the Federal University of Technology, Minna, Nigeria, and the Ph.D. degree in electronic and computer systems engineering from the Victoria University of Wellington, New Zealand. He is currently an Assistant Professor with the Wireless Communication Networks (WCN) Section, Aalborg University, Denmark. Since 2020, he has been an External Research Engineer with Nokia Bell Labs, Aalborg. Prior to joining Aalborg University, he also worked in various positions at the University of Cape Town, South Africa; Odua Telecoms Ltd., Nigeria; Izon Science Ltd., Christchurch, New Zealand; and National Space Research and Development Agency, Nigeria. He has coauthored over 40 international publications, including conference proceedings and journal contributions. His research interests include channel characterization, machine learning and AI for communications, radio resource allocation, intelligent spectrum access, and interference management.

ISABEL DE-LA-BANDERA received the M.Sc. and Ph.D. degrees in telecommunication engineering from the University of Malaga. In 2010, she joined the Department of Communications Engineering, University of Malaga. She has participated in many projects, national and international, and concerning radio resource management in mobile networks. She has also collaborated with major mobile operators and vendors and participated in the H2020 ONE5G Project. She is currently participating in the H2020 LOCUS Project.

RAQUEL BARCO received the M.Sc. and Ph.D. degrees in telecommunication engineering. She has worked at the Telefónica and the European Space Agency. She is currently a Full Professor with the University of Malaga. She participated at the Mobile Communication Systems Competence Center, jointly created by Nokia and the University of Malaga. She has published more than 100 scientific papers, filed several patents, and led projects with major companies, and participated in the H2020 ONE5G Project. She is currently participating in the H2020 LOCUS Project.